Potentialities of the finite element method in electromagnetic tomography

∗ Victor Cezar Tocantins de Souza (vsouza@ufpa.br). Luiz Rijo (rijo@amazon.com.br). UFPA/CPGF, Brazil

Abstract

Geophysical electromagnetic data are usually analyzed using forward and inverse modeling techniques. For the forward modeling the finite element method has been used successfully due its facility to handle geological structures with arbitrary shapes. The inverse modeling is usually done with constrained Marquardt algorithm.

The purpose of this paper is to show the potentialities of the finite element method in electromagnetic tomography forward problem using complex geological models with azimuthal symmetry. Equality constrains in the inverse problem have greatly improved the recovered image. Three factors are analyzed: the resolution of recovered image as a function of frequency, the effect of contrasts between the anomalous bodies and the homogenous background and the response of models with complex geometries. All studied examples show excellent results.

Introduction

Recently electromagnetic (EM) tomography has received special attention from geophysical community. Indeed, applications of this tool have been used in development and characterization of petroleum reservoirs. Even though images with high-resolution have been previously produced by techniques of cross-well seismic tomography, EM tomography has brought additional geological information from reservoir, through analyzes of the distribution conductivity subsurface, such as: rock porosity, fluid saturation and fracture orientation. Although, some progress in EM tomography has already been accomplished, improvements still needed to be done in order to get better imaging resolution from the subsurface.

The interpretative modeling of the EM tomography can be divided in two parts; the forward problem, where the EM data are computed by solution of the differential equation that governs the model, and a second part, called of the inverse problem, where the EM data are inverted through techniques of geophysical inversion in order to obtain the electrical conductivity distribution of model. Thus, improved techniques of modeling in forward problem or inversion methods bring news potentialities in EM tomography.

Within the last years, important progress had been made in cross-well EM tomography. Nekut introduced ray-trace modeling (Nekut, 1994). Alumbaugh and Morrison have shown an iterative Born approach to EM tomography (Alumbaugh and Morrison, 1995). Newman (Newman, 1995) formulated an inverse solution using integral and differential equations.

This paper presents the potentialities of finite element method in forward modeling of EM tomography through of interpretative geological models with azimuthal symmetry. The inverse problem is solved by the Marquardt method, introducing equality constrains as priori information (Souza et al., 2001), following the formulation introduced by Medeiros and Silva (Medeiros and Silva, 1996). The models with azimuthal symmetry are adequate to represent plumes of gas or fluid that are injected in enhanced recovery process, principal area of application of cross-well techniques in oil industry.

The versatility of the proposed method are illustrated in simple models introduced by Alumbaugh and Morrison (1995) and for additional sophisticated models whereas the complex geometries are explored.

Forward problem

The finite element method has been successfully applied in modeling of electrical and EM geophysical problems (Coggon, 1971), (Rijo, 1977) and (Pridmore et al., 1981). This method can be used to solve the differential equations with its boundary conditions associated, which describe the behavior of electrical and EM fields in subsurface. The main advantage of the method is the facility of incorporating complex geometries in interpretative models that represent the geological environment. Thereby, this method becomes a powerful tool to solve electromagnetic cross-well problems, where we are interested in high-resolution images of inter-well region containing distribution of physical proprieties with complicated geometries.

The governed equation is the Helmholtz equation, applicable to cylindrical with azimuthally symmetric geometry about vertical magnetic dipole sources. This assumption reduces the 3D vector forward problem to a manageable 2D scalar form. Taking a cylindrical coordinate reference system (r, θ, z) with the z-axis pointing downward. Our models consist of cylindrical anomalous in an otherwise homogeneous background of electrical conductivity σ^p. Vertical magnetic dipole sources are laid upon the symmetric axis that represents a well. One example of this geometry is the classical model introduced by Alumbaugh, (Alumbaugh and Morrison, 1995), as is shown in Figure 1. This represents two three-dimensional sectioned anomalous cylindrical targets embedded in a homogeneous medium.

Because of cylindrical symmetry imposed upon the interpretative model and the kind of the sources used, the forward problem exhibits pure transverse electric (TE) mode, thus existing only the transversal electric field, E_θ.

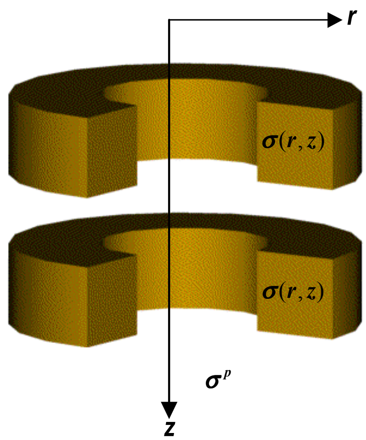

Figure 1 – Cylindrical geometry for electromagnetic tomography. The anomalous bodies are cylindrically about the magnetic dipole sources.

Following Ward and Hohmann (Nabighiam, M. N., Ed., 1988), the transversal electric field can be decomposed as the sum of a primary field, due by homogeneous background, that has analytical solution, and in a secondary field due to the anomalous bodies around of the sources.

Assuming a harmonic temporal dependence $e^{-i\omega t}$, the differential equation resultant for the secondary transversal electric field has the form.

$$-\frac{\partial}{\partial z}\left(\frac{1}{\hat{z}}\frac{\partial E_\theta^s}{\partial z}\right)-\frac{\partial}{\partial r}\left(\frac{1}{\hat{z}}\frac{1}{r}\frac{\partial (rE_\theta^s)}{\partial r}\right)+\hat{y}E_\theta^s=-\Delta\hat{y}E_\theta^p \qquad (1)$$

where $\hat{y}=\sigma$ is the admittivity, $\hat{z}=i\omega\mu$ is the impedivity, $\Delta\hat{y}=\hat{y}-\hat{y}^p=\sigma-\sigma^p$ is the difference between the admittivity of anomalous bodies and of the homogenous background.

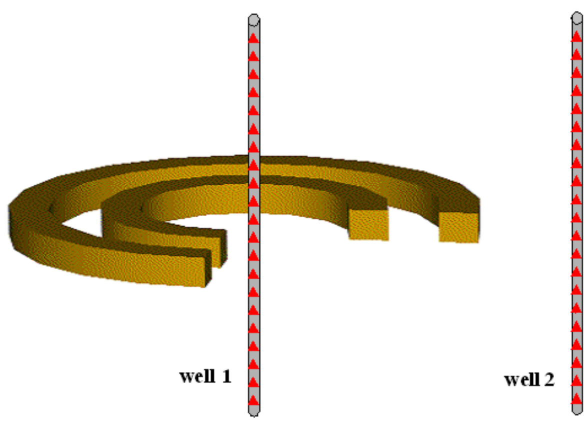

Figure 2 – Wells frame for electromagnetic tomography. The sources are located in well 1, whereas in well 2 are located the receivers.

After we get to solve numerically the equation (1), the vertical components of magnetic fields H_z are computed in the receivers in another parallel well. This situation is illustrated in Figure 2, (Alumbaugh and Morrison, 1995). The relationship between the transversal electrical field and the vertical magnetic field has the form.

$$H_z=-\frac{1}{\hat{z}}\frac{1}{r}\frac{\partial (rE_\theta)}{\partial r} \qquad (2)$$

As the vertical component of magnetic field can be obtained by numerical differentiation, the main effort in the forward modeling is to solve the equation (1) through of numerical techniques.

Finite element formulation

The finite element method is a numerical technique for obtaining approximate solutions to boundary value problem. It consist in discretize the domain of differential equation in fundamental elements, the finite elements, and approaches the solution to an interpolation of simple function, the basis functions.

As we are working with a model that presents azimuthal symmetry, we can consider only a slice of the three-dimensional region, hence the domain becomes bi-dimensional. The Figure 3 illustrates a transversal section of the region limited by wells. It is divided in triangular elements with conductivity constant in each element. Because the homogenous Dirichlet boundary conditions have to be satisfied, the discretized region extends beyond of the area limited by the two wells, where the EM fields can be considered negligible at border of the domain. At the sources well Newman condition has to be used.

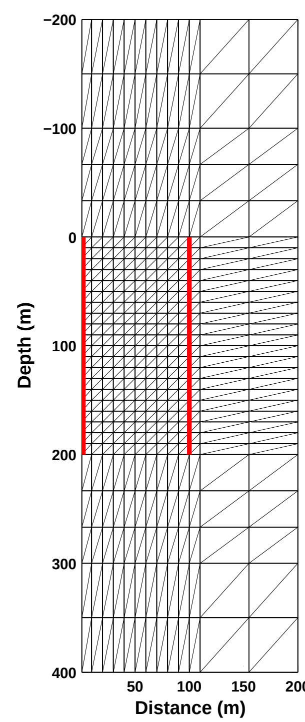

Figure 3 – Region discretized for the finite element formulation. The anomalous bodies are present in the area limited by wells.

Inverse process

The interpretative model takes fundamental role in the inverse process. Since the original 3-D model was reduced for a bi-dimensional model, Our interpretative model consists of an inter-well region discretized into cells. Each cell is formed by two triangular finite elements and inside each of then, the electrical conductivity is constant. The numerical values of electrical conductivity are the parameters to be estimated in the inverse process. The vertical magnetic fields measured at receivers compose the observed data. Using only an adjusting functional that expresses the relationship between this data and the parameters of the interpretative model results in an ill-posed inverse problem (Medeiros and Silva, 1996). Hence we should to add priori information in order to transform an ill-posed problem into a well-posed problem.

In this work we add equality constrains about the electrical conductivity of background and about cells that surround the interpretative model. For the first guess in the inverse process, we use the conductivity of the uniform host. This approach has been applied to invert resistivity and electromagnetic data (Constable et al., 1987; deGroot-Hedlin and Constable, 1990; Wang et al., 1994). The equality constrain incorporated in the cells are absolute constrains, that is, each parameter is required to be as close as possible to a typical numerical values. These values can be obtained through rock analysis sample or by another geophysical method.

Have handled the equality constrains described previously, we can add it into the inverse process through the Lagrange multipliers, in order to obtain a stabilized functional. Thus the resultant functional is minimized in least-square sense employing the iterative Marquardt algorithm. The estimated parameters are obtained when the current parameters produce data that fit with the observed data, unless the variance of noise presents in the data. This condition corresponds in a minimal point of stabilized functional.

Results

In this section we illustrate through recovered images of synthetic data the potentialities of the finite element method in EM tomography. We analyze the following aspects: frequency resolution, arrangement of the target (anomalous bodies), conductivity contrasts and mainly complex geometries.

The first result illustrates the resolution as a function of frequency for the classical model introduced by Alumbaugh, (Alumbaugh and Morrison, 1995), as shows the Figure 4a. This is a model that allows measuring of the vertical resolution of the employed method, since we have two anomalous bodies arranged vertically embedded in a homogenous background. The model presents two 20 x 20 m conductive blocks of 0.02 S/m separated by 20 m in a 0.01 S/m whole space. Were used 21 sources and 21 receivers spaced at 10 m intervals in the 200 m deep wells. The receivers well is distanced 100 m from the well that contains the vertical dipole sources. In the inverse process the vertical magnetic fields measured at receivers compose the observed data.

In order to simulate real data in the inverse process, the synthetic data were corrupted with pseudo-random Gaussian noise with zero mean and variance of 5% of the minimum total magnetic field. The inverse problem is stabilized adding the equality constrains described in the previous section. We assume to known the true value of the conductivity background unless a certain degree of uncertainty. This assumption it is not a strong priori-information, since we can obtain it easily from well logging data.

Figures 4b through 4f illustrate the recovered images from model showed in Figure 4a. We notice that the resolution of the recovered images improves with increasing of the frequency. Obviously there is a limit determined by the skin depth effect. We see that at 1 kHz there is no response to the targets at all, for 10 kHz, already is possible to distinguish the two anomalous, but the resolution is poor. At 100 kHz the targets bodies are well visible and finally at frequency of 300 kHz the recovered image presents high resolution, and hence approach it of the true model.

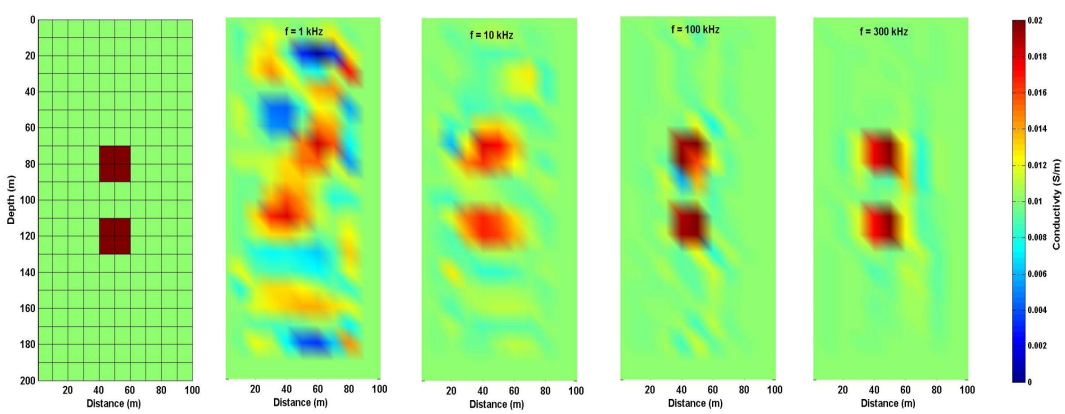

(a) (b) (c) (d) (f)

Figure 4 - Results for two anomalous bodies vertically separated in four frequencies. (a) True model, - recovered image - at: (b) 1 kHz, (c) 10 kHz, (d) 100 kHz and (f) 300 kHz.

The model exemplified previously is not adequate for analyzing horizontal resolution. A model that is better suited for describing the lateral resolution is shown in Figure 5a. In this case the two 0.02 s/m blocks are separated horizontally by 20 m in a 0.01 S/m background.

Instead of make simulations in many frequencies, and analyzing the recovered images for a determined model, we choose to analyze the recovered images for a model containing three levels of conductivity contrasts. Thus we can analyze both the horizontal resolution and the effects of different degree of conductivity contrasts. The Figure 5b illustrates the result at 100 kHz for the true model illustrated in Figure 5a. We notice the two targets are recovered with high resolution.

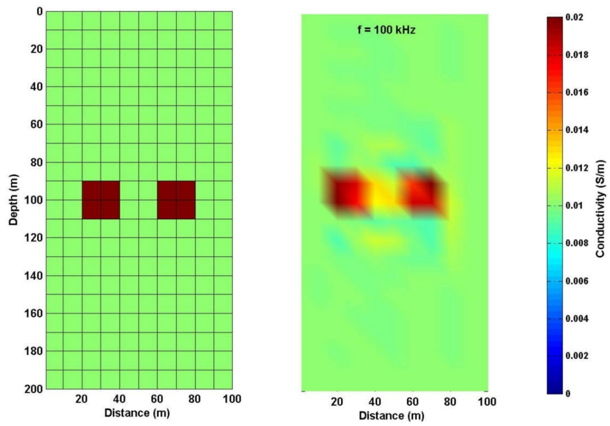

(a) (b)

Figure 5 - Results at 100 kHz for two anomalous bodies horizontally separated, where the conductivities are twice greater than of the homogeneous background, (a) true model (b) recovered image.

In Figure 6a the conductivity of the targets are four times greater than the background. Using a frequency of 300 kHz we obtain a recovered image that approaches to the true model, as is shown in Figure 6b.

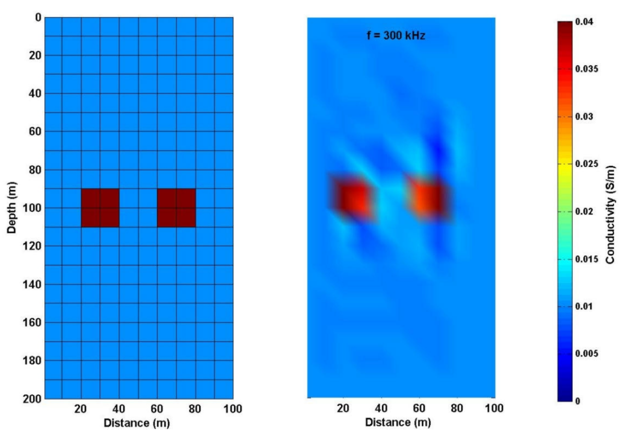

(a) (b)

Figure 6 - Results at 300 kHz for two anomalous bodies horizontally separated, where the conductivities are four times greater than of the homogeneous background, (a) true model (b) recovered image.

Using a frequency of 50 kHz for the true model illustrated In Figure 7a, where the conductivity of the targets are six times greater than the background. We obtain a recovered image with high resolution, as is shown in Figure 7b

In fact, for the three cases we notice that there is not overlap between the anomalous bodies. This is a grateful characteristic of the responses produced by the finite element method, where different arrangements of the targets not influence the lateral resolution.

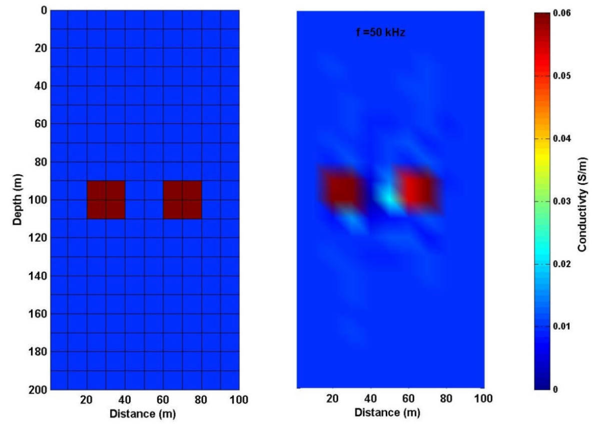

(a) (b)

Figure 7 - Results at 50 kHz for two anomalous bodies horizontally separated, where the conductivities are six times greater than of the homogeneous background, (a) true model (b) recovered image.

It was illustrated that the finite element method yielded to good recovered images for targets arranged vertically and horizontally. This fact leads to models that own complex geometries. For example, The Figure 8 illustrates four targets taking shape of the acronym **SbgF**. A slice of this model reveals targets with complicated geometries.

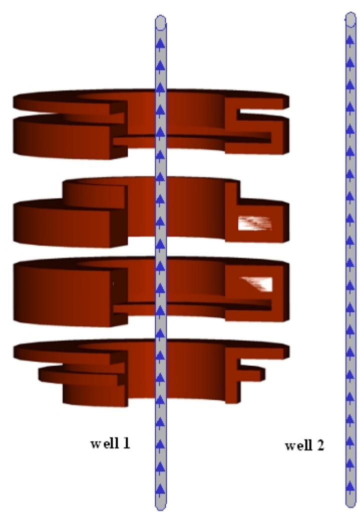

Figure 8 – Three-dimensional representation of complex geometry. A section of anomalous bodies between the wells show us the acronym – **SbgF**.

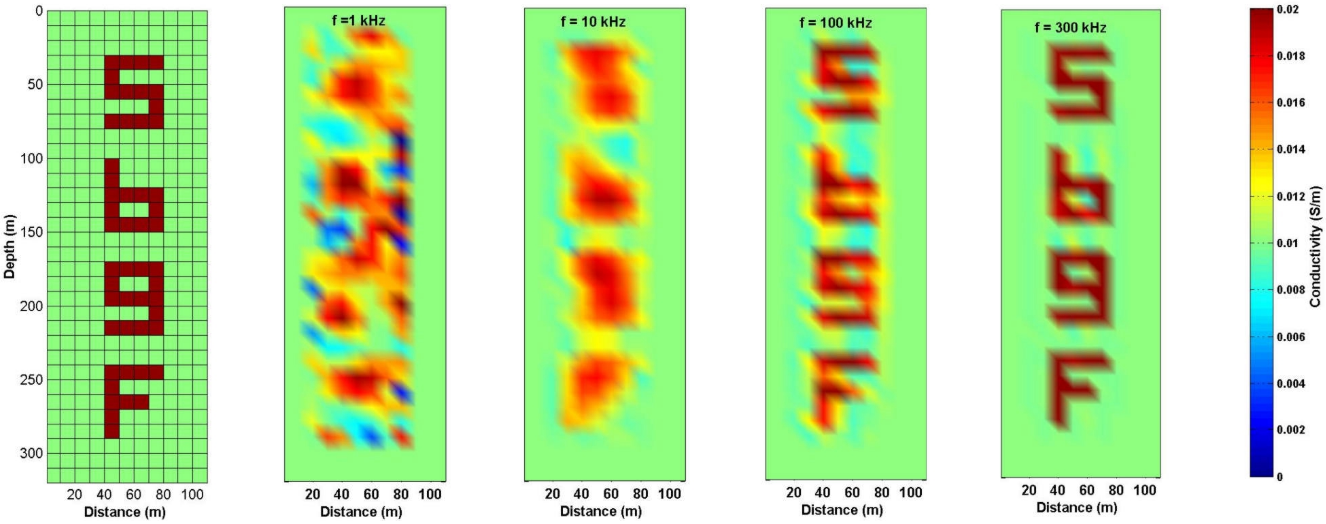

(a) (b) (c) (d) (e)

Figure 9 - Results for anomalous bodies with complex geometries four frequencies. (a) True model, - recovered image - at: (b) 1 kHz, (c) 10 kHz, (d) 100 kHz and (f) 300 kHz.

The Figure 9a shows the 2D section of the three-dimensional model illustrated in Figure 8. The Figures 9b through 9f display the results using four frequencies. At 1 kHz it is not possible distinguish the targets; due to the low-resolution resultant, as illustrates the Figure 9b. Increasing the frequency to 10 kHz we notice which the anomalous take shapes in four bodies, but the details of the targets are not displayed, as is shown in Figure 9c. At 100 kHz the details already are noticed, this improvement of the resolution is displayed in Figure 9d. If the frequency is increased for 300 kHz the recovered image approaches of the true model, as illustrates the Figure 9e.

We showed that the recovered images present high resolution, when is used an appropriate frequency, however this accuracy can be counted through the error between the true and recovered models.

The Figure 10 illustrates the relative errors for the recovered images showed in Figure 9. The Figures 10a through 10d display the presence of constrains around of image and how the relative error decreases gradually with increasing of the frequency and consequently of the resolution.

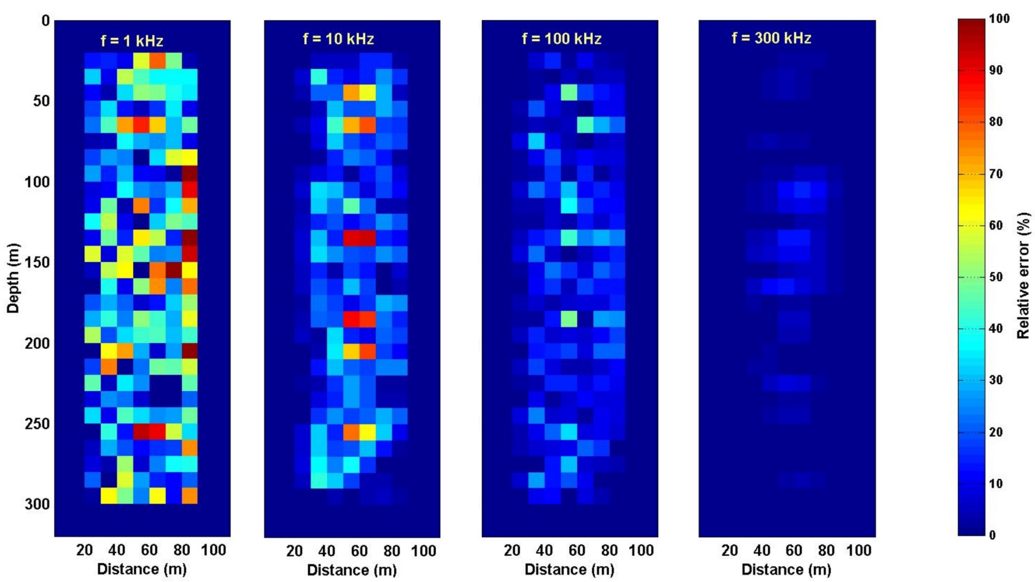

(a) (b) (c) (d)

Figure 10 - Results for the relative errors of the recovered images illustrated in Figure 9, (a) at 1 kHz, (b) 10 kHz, (c) 100 kHz and (d) 300 kHz.

Conclusions

We presented the potentialities of the finite element method in electromagnetic tomography analyzing three factors: the resolution of recovered image as a function of frequency, the effect of the contrasts between the targets and the homogenous background and last the response for model that explores complex geometries.

The approach using the finite element method produces image with high resolution in higher frequencies. As it has been demonstrated in other approach methods introduced for EM tomography, such as Born and Rytov schemes. Although the rate of attenuation at these frequencies can cause serious problems of stability with respect the inverse problem, due to the magnitude of the data become very small.

We illustrated through of several examples that for great contrasts between the conductivities of the targets and of the background, we got good inter-well images. This, because the finite element method doesn't work with approaches the first or second order for the governed differential equation, thus we can handle diverse level of contrast directly, in contrast to the first order approaches usually used in Born and Rytov scheme.

Finally, we should state that the main attractive of the method introduced in this paper, it is the facility in incorporate complicated geometries into interpretative model, it has been showed that the finite element method demonstrated high capacity of the resolution for targets that posses complex shapes.

References

Alumbaugh, D. L., Morrison, H. F., 1995, Monitoring subsurface changes over time with cross-well electromagnetic tomography: Geophysical Prospecting,, 430, p 873 -902.

Alumbaugh, D. L., Morrison, H. F., 1995, Theoretical and practical considerations for crosswell electromagnetic tomography assuming a cylindrical geometry: Geophysics, vol. 60, No. 3, p 846 -870.

Coggon, J. H., 1971, Electromagnetic and electrical modeling by finite element method: Geophysics, vol. 36, No. 1, p 132 -155.

Constable, S. C., Parker, R. L., and Constable, C. G., 1987, Occam's inversion: A practical algorithm for generating smooth models from electromagnetic sounding data: Geophysics, vol. 52, p 289–300.

Medeiros, W. E., Silva, J. B. C., 1996, Geophysical inversion using approximate equality constraints: Geophysics, vol. 61, No. 6, p 1678 -1688.

Nabighiam, M. N., Ed., 1988, Electromagnetic methods in applied geophysics 1, theory: Soc. Expl. Geophys.

Nekut, A. G., 1994, Electromagnetic ray-trace tomography: Geophysics, vol. 59, No. 3, p 371 -377.

Newman, G., 1995, Crosswell electromagnetic inversion using integral and differential equations: Geophysics, vol. 60, No. 3, p 899 -911.

Pridmore, D. F., Hohmann, G. W., Ward S. H., and Sill, W. R., 1981, An investigation of finite – element modeling for electrical and electromagnetic data in three dimensions: Geophysics, vol. 46, No. 7, p 1009 -1024.

Rijo, Luiz., 1977, Modeling of electro and electromagnetic data: PhD thesis, Department of geology and Geophysics, University of Utah, Salt Lake City, Utah, USA.

Souza, V. C. T., Baptista, J. J. and Rijo, L., 2001, Electromagnetic tomography using absolute constrains, 7th International Congress of The Brazilian Geophysical Society, Salvador, in CD-ROM.

Wang, T., Oristaglio, M., Tripp, A., and Hohmann, G. W., 1994, Inversion of diffusive transient electromagnetic data by a conjugate-gradient method: Radio Science, 29, 1143–1156.

Acknowledgments

This work was supported by program ANP/FINEP-UFPA and CTPETRO/CNPq-46295/00-8. The authors would like to thank to Curso de Pós-Graduação em Geofísica – UFPA for logistic support and to all researchers this department.